

Three-dimensional stability of the solar tachocline

Rainer Arlt, Aniket Sule, Günther Rüdiger

Astrophysikalisches Institut Potsdam, An der Sternwarte 16, Germany

February 7, 2005

Abstract. The three-dimensional stability of the tachocline is investigated.

1. Motivation

Helioseismology has provided us with information on the internal rotation of the Sun. The angular velocity depends on latitude as well as radius. The dependence is mainly a latitudinal in the bulk of the convection zone, whereas the solar radiative core rotates nearly uniform with an angular velocity of the convection zone at about 30° latitude. The transition from the differential rotation in the convection zone to the uniform rotation in the core is thin – probably thinner than 5% of the solar radius – and is called the tachocline.

The convection zone is thermally overcritical and the stability of shear flows is not an issue there. The shear in the tachocline however is latitudinal and radial and may be subject to shear-flow instabilities. If the tachocline is turned into a turbulent layer, a problem arises with the mixing of elements, most notably with Lithium which will be destroyed in nuclear fusion up to 0.68 solar radii (R_\odot), just below the convection zone. A turbulent tachocline mixing the Lithium into its fusion zone would contradict the observed relatively high Lithium abundance at the surface of the Sun.

The situation in the solar tachocline was described by Spiegel & Zahn (1992) as exhibiting horizontal turbulence, excited by hydrodynamic shear-flow instability. It was argued that the two-dimensional turbulence provides angular momentum transport but inhibits too strong mixing of Lithium below $0.68R_\odot$.

The hydrodynamic stability of the latitudinal shear in the tachocline was studied by Watson (1981). The dependence on colatitude θ was $\Omega = \Omega_{\text{eq}}(1 - \alpha_2 \cos^2 \theta)$, where Ω_{eq} is the equatorial angular velocity at the bottom of the convection zone and α_2 is a parameter for the relative equator-to-pole difference of the angular velocity. Watson found instability for a differential rotation with $\alpha_2 > 0.286$. Unfortunately, this is in the vicinity of the value of solar differential rotation, and the result was not definitely deciding between a turbulent and a stable tachocline. The investigation was two-dimensional argu-

ing that the stable stratification will not allow significant radial flows, but thereby the radial shear is neglected, too.

Charbonneau et al. (1999a) extended the linear stability analysis to various rotation profiles of the form

$$\Omega = \Omega_{\text{eq}}(1 - \alpha_2 \cos^2 \theta - \alpha_4 \cos^4 \theta). \quad (1)$$

Different layers of the tachocline were associated with different results from helioseismology in terms of α_2 and α_4 . The upper layer which is thought to be penetrated by convective overshooting was found to be unstable to the shear, whereas the lower layer with smaller latitudinal shear turned out to be stable.

Garaud (2001) investigated the weakly non-linear behaviour of this horizontal instability and found the overcritical system developing into a marginal state very close to the observed rotational profile.

In order to address the entire tachocline and since the tachocline is a place where latitudinal and radial shear meet, we investigate the stability of the three-dimensional rotation profile. Although it is very reasonable to assume that radial flows will be weak, the variation of the latitudinal differential rotation with radius across weakly coupled spherical layers could provide different results for the stability of the tachocline. We will briefly summarize the numerical background in Section 2, provide details of the computational results in Section 3, and summarize our findings in Section 4.

2. Computational setup

The rotational profile depends on both latitude and radius in this study. Between the inner and outer radius of the tachocline, $r_i = 0.65$ and $r_o = 0.7$ respectively, the angular velocity is defined by

$$\Omega(r, \theta) = \Omega_{\text{eq}} \left[1 - \alpha_2 \cos^2 \theta - \alpha_2 \left(\frac{1}{4} - \cos^2 \theta \right) \frac{r_o - r}{r_o - r_i} \right], \quad (2)$$

where θ denotes the colatitude in the spherical shell, r is the radial coordinate, and Ω_{eq} is the equatorial angular velocity. The profile implies that the rotation velocity at

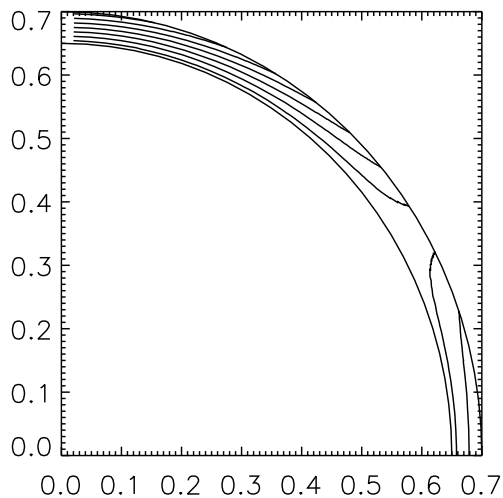


Fig. 1. Vertical cross-section through the solar tachocline with contours of the assumed angular velocity depending on radius and latitude as given by (2). Highest angular velocity is at the equator (bottom right), and radially constant rotation occurs at a heliographic latitude of 30° .

the inner boundary of the computational domain, $r = r_i$, is the one at $\theta = 60^\circ$ (or 30° heliographic latitude). This appears to be a valid assumption in agreement with various helioseismological inversions (recently e.g. Schou et al. 2002), whereas core rotation may be adopted at larger latitudes higher up in the convection zone.

We employ the incompressible, viscous Navier-Stokes equation and linearize the problem. We can then separate the axisymmetric background rotation \mathbf{U} from the non-axisymmetric flow \mathbf{u} . The latter is evolved by numerical computations. The normalised equation of motion reads

$$\frac{\partial \mathbf{u}}{\partial t} = \mathbf{u} \times \nabla \times \mathbf{U} + \mathbf{U} \times \nabla \times \mathbf{u} - \nabla p - \nabla(u \cdot \mathbf{U}) + \Delta \mathbf{u}, \quad (3)$$

and the continuity equation $\nabla \cdot \mathbf{u} = 0$ holds. The equation is evolved with the spectral spherical code by Hollerbach (2000). The actual integration employs the radial components of the curl and the curl-curl of the equation, thereby eliminating the gradient terms.

The normalisation of the equation with the viscous time $\tau_\nu = r_o^2/\nu$ and the length scale r_o leads to the Reynolds number

$$\text{Re} = \frac{r_o^2 \Omega_{\text{eq}}}{\nu} \quad (4)$$

as a free parameter which is essentially a variation of the viscosity ν since radius and Ω_{eq} are sufficiently well known. The solar Reynolds number in the tachocline is – in terms of the definition of (4) – about 10^{14} . We try to achieve time series for numerically demanding $\text{Re} > 10^4$. By comparison with known results from inviscid two-dimensional analyses, we find that the critical viscous differential rotation at $\text{Re} > 10^3$ or 10^4 is already sufficiently close to the inviscid value.

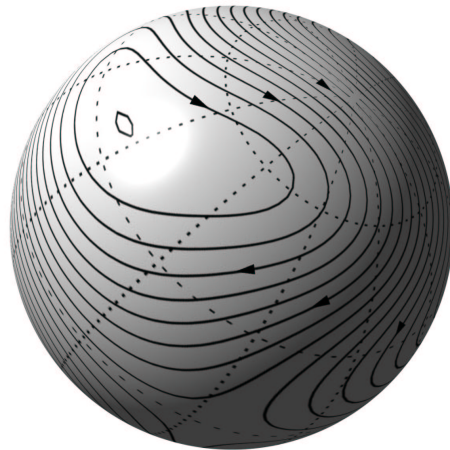


Fig. 2. Streamlines of the symmetric eigen function of the computation with a three-dimensional profile $\Omega(r, \theta)$ on the surface of the tachocline at $r = 0.7$. Flows are strongest through the poles (top right). Two circulation cells are found on each hemisphere.

The velocity is decomposed into poloidal and toroidal potentials, and those are again decomposed into radial Chebyshev polynomials and spherical harmonics. Since the potentials are evolved, the continuity equation is fulfilled automatically. The density is constant throughout the computational domain. In a thin shell of 5% of the solar radius, this is a reasonably good approximation of the true situation. We also do not take any deformation of the tachocline into account. Top and bottom radius of the tachocline are constant over latitude. Charbonneau et al. (1999b) found a prolate tachocline whose equatorial part is located at slightly smaller radius than the polar end. We assume that the difference of 3.5% in location of the tachocline has negligible effect on the results, but may be an issue of future investigations.

The radial boundary conditions are stress-free at both r_i and r_o . At Reynolds numbers of $\text{Re} > 10^4$, high spectral resolution was necessary to obtain reliable results. Up to 80 Chebyshev and 80 Legendre polynomials were used to resolve the flow properly.

The azimuthal modes of the problem described by (3) are decoupled, and we can study the stability of individual m -modes separately. Moreover, even and odd latitudinal modes (symmetric and antisymmetric modes with respect to the equator) decouple, and we will have a look into the critical differential rotation for the excitation of instability of the two kinds separately. The radial modes all couple and do not provide results on the stability of individual radial wavelengths.

3. Results

3.1. Stability of various solutions

In a set of fiducial computations, we applied a purely latitudinal profile of the angular velocity. An $m = 1$ mode is evolved with the profile of (1) where $\alpha_4 = 0$ and α_2

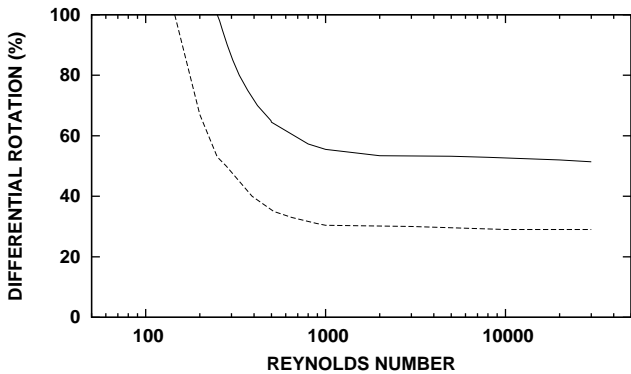


Fig. 3. Lines of marginal stability for the combined latitudinal and radial shear (solid line) and the purely latitudinal shear (dashed line). Differential rotation denotes the percentage by which the pole's angular velocity is slower compares with the equatorial one.

is varied. Since we solve a viscous problem, the critical differential rotation, α_2^{crit} , depends on the Reynolds number. The result is already very close to Watson's inviscid result for $\text{Re} \geq 1000$. This is good reason to assume that the numerical solutions reaching $\text{Re} \sim 30\,000$ are suitable approximations for the solar plasma.

Despite allowing for radial motions, the evolution provides solutions which are nearly toroidal and do not show significant radial flows. They are surface flows forming two cells on each hemisphere with stream lines through the poles. Figure 2 shows a representation of the flow in the spherical surface. The graph has to assume that the poloidal component of the velocity is zero though, which is not entirely true.

The second step involved the rotation profile of (2) for which the critical steepness of the differential rotation, α_2^{crit} , is again sought for various Reynolds numbers. Figure 3 shows the lines of marginal stability, i.e. the critical differential rotation, versus Reynolds number for the symmetric $m = 1$ mode. The solid line refers to profile (2), the dashed line is the latitudinal profile and converges to the result by Watson (1981) for $\text{Re} \rightarrow \infty$.

The most easily excited patterns of $m = 1$ are always symmetric with respect to the equator. We can also look for the stability of antisymmetric patterns and find the results shown in Figure 4. They are more stable than the symmetric configurations with an $\Omega(r, \theta)$ profile. The antisymmetric solutions from the $\Omega(\theta)$ profile have also higher critical differential rotation values than their symmetric counterparts.

The patterns drift with a certain velocity in azimuthal direction. Since the equations hold for the nonrotating system, we can directly convert the pattern rotation into physical times. The pattern rotation period for the two-dimensional and the three-dimensional profile of Ω is shown in Figure 5 by a dashed and a solid line, respectively. The actual rotation periods are also plotted. The reference equatorial period of 25.44 d ($\Omega_{\text{eq}} = 455$ nHz) is given as dash-dot line. The pattern rotation periods are

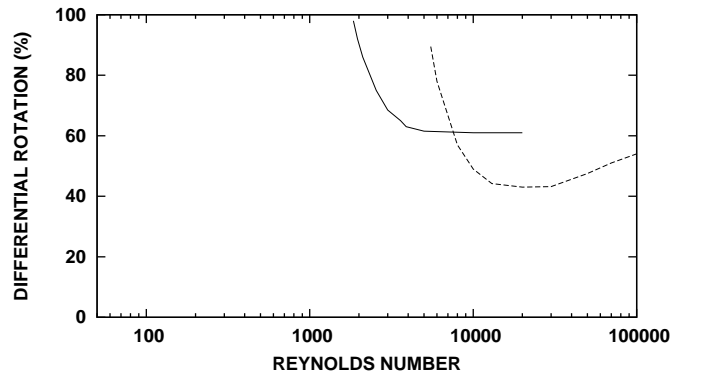


Fig. 4. Lines of marginal stability for the antisymmetric $m = 1$ solutions caused by the combined latitudinal and radial shear (solid line) and the purely latitudinal shear (dashed line).

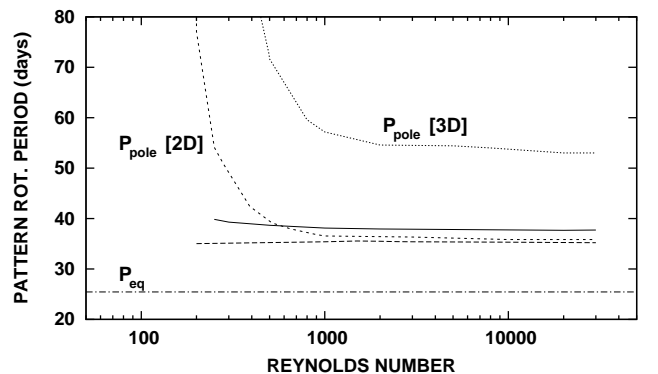


Fig. 5. Rotation period of the flow pattern for the two-dimensional (dashed) and the three-dimensional (solid) rotation profile. The numbers are computed assuming an equatorial rotation period of 25.44 d ($\Omega_{\text{eq}} = 455$ nHz) which is plotted with a dash-dot line. Periods are computed at marginal stability; the polar rotation period for this critical differential rotation is plotted as short-dashed and dotted lines for the 2D and 3D cases, respectively.

determined at marginal stability. Since the marginal case gives us a value for the differential rotation, we also plot the polar rotation period P_{pole} versus Re . The short-dash line is for the two-dimensional $\Omega(\theta)$ -profile, the dotted line is for the three-dimensional case described by (2).

The pattern rotation periods are always between the equatorial and polar rotation periods, in agreement with the 2D results by Charbonneau et al. (1999a). While the patterns from the 2D- Ω profile are close to the polar rotation period, the patterns rotate with nearly the average rotation period between the polar and equatorial ones.

We can compute the time after which the pattern is passes by a given point on the equator. This time is often called lap time. Assuming an equatorial rotation period of 25.44 d ($\Omega_{\text{eq}} = 455$ nHz), we find a lap time of 91 d for the 2D case, and a lap time of 78 d for the 3D case.

Modes with higher azimuthal mode numbers require significantly higher differential rotation for instability. The antisymmetric $m = 2$ mode which is symmetric with respect to the equator was found to be stable even in the

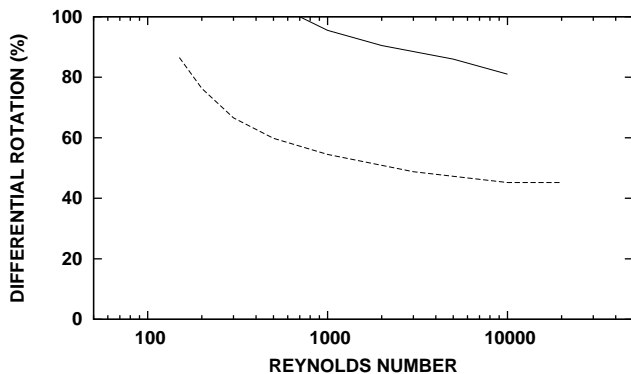


Fig. 6. Lines of marginal stability for the antisymmetric $m = 2$ mode resulting from the combined latitudinal and radial shear (solid line) and the purely latitudinal shear (dashed line).

entire parameter range covered by Fig. 3. This is in agreement with the inviscid, two-dimensional stability analysis by Charbonneau et al. (1999a). The stability lines for the antisymmetric $m = 2$ mode are shown in Fig. 6. We could not find instability for any $m = 3$ mode in the range covered by Fig. 3.

3.2. Effects of buoyancy

Little influence is expected from the stable temperature gradient in the tachocline. Since we do have the chance to prove this in our three-dimensional simulations, we demonstrate the effect of a negative buoyancy force on the stability of the differential rotation. The Navier-Stokes equation is extended by the buoyancy force and reads in the non-dimensional form:

$$\frac{\partial \mathbf{u}}{\partial t} = \mathbf{u} \times \nabla \times \mathbf{U} + \mathbf{U} \times \nabla \times \mathbf{u} + \text{Ra} \Theta \mathbf{r} - \nabla p - \nabla(\mathbf{u} \cdot \mathbf{U}) + \Delta \mathbf{u}, \quad (5)$$

$$\frac{\partial \Theta}{\partial t} = -\mathbf{U} \cdot \nabla \Theta - \mathbf{u} \cdot \nabla T + \frac{1}{\text{Pr}} \Delta \Theta, \quad (6)$$

with a background temperature profile of

$$T = \frac{r_i}{r_o - r_i} \left(\frac{r_o}{r} - 1 \right) \quad (7)$$

and the Prandtl number being the ratio between viscosity and thermal diffusivity, $\text{Pr} = \nu/\chi$. The Rayleigh number in (6) is

$$\text{Ra} = \frac{g\alpha(T_i - T_o)r_o^3}{\nu^2}, \quad (8)$$

where g is the gravitational acceleration, α is the coefficient of volume expansion, and T_i and T_o are the temperatures at the two boundaries. In the Boussinesq formulation used here, the presence of a sub-adiabatic temperature gradient actually translates into a negative value of Ra. We set our version of the Rayleigh number to a value as small as $\text{Ra} = -10^8$ in order to see any notable effect on the flow. The Prandtl number is set to unity.

The critical differential rotation for a growing symmetric $m = 1$ mode at $\text{Re} = 10^4$ increases slightly to 53.3%

as compared with the non-buoyant value of 52%. This is in line with the fact that the solutions contain nearly horizontal motions.

4. Summary

A fully three-dimensional, linear analysis of the stability of the solar tachocline was carried out. If radial variation of the angular velocity is included in the model, the maximum pole-equator difference of the angular velocity can be as large as 52%. It is not radial flows emerging from the extension in the third dimension, but it is changed stability conditions emerging from the radial shear and radial dependence of the differential rotation.

Other modes such as higher m or different flow symmetries do not get unstable at lower critical differential rotation values under the influence of a three-dimensional rotation profile.

The stabilizing effect of the temperature gradient has been proven, but since all the unstable modes are very nearly horizontal, the influence is small. The assumption that horizontal motions dominate is valid even without a stabilizing temperature gradient. However the assumption that spherical shells of infinitesimal thickness do not interact with each other is not applicable, according to our results. One may argue that the viscosity in the computer simulations is much too high, but the variation of the results is very small at $\text{Re} > 1000$. This is an indication that computations with $\text{Re} = 10^4$ or higher are a good approximation of the near-inviscid solar case. We conclude that all parts of the tachocline not being affected by convective overshooting are stable.

References

- Charbonneau, P., Dikpati, M., Gilman, P., 1999a, ApJ 526, 523
- Charbonneau, P., Christensen-Dalsgaard, J., Henning, R. et al., 1999b, ApJ 527, 445
- Garaud, P., 2001, MNRAS 324, 68
- Hollerbach, R., 2000, Int. J. Numer. Meth. Fluids 32, 773
- Schou, J., Howe, R., Basu, S. et al., 2002, ApJ 567, 1234
- Spiegel, E.A., Zahn, J.-P., 1992, A&A 265, 106
- Watson, M., 1981, GAFD 16, 285